Iranian Journal of Medical Physics
ijmp.mums.ac.ir

Optimization of Dose and Image Quality in Full-fiand Computed Radiography Systems for Common Digital Radiographic Examinations

Soo-Foon Moey [1*], Zubir Ahmad Shazli[1]

1. Department of Diagnostic Imaging and Radiotherapy, Kulliyyah (Faculty) of Allied Health Sciences, International Islamic University Malaysia, Kuantan Campus, 25200 Kuantan, Pahang, Malaysia

ARTICLE INFO

Article type:
Original Article

Article history:
Received: Jul 21, 2017
Accepted: Oct 27, 2017

Keywords:
Digital Radiography
Radiation Monitoring
Radiation Protection
X-Ray

ABSTRACT

Introduction: Optimization facilitates image quality and radiation dose by minimizing stochastic and deterministic effects. This study was to obtain images of acceptable quality with no harmful effects for common radiographic examinations in digital imaging.

Materials and Methods: This study was conducted in three phases. The pre-optimization phase involved 90 physically able patients weighing 60-80 kg and aged 20-60 years. The estimation of dose and image quality was performed on four common digital radiographic examinations. The entrance surface dose (ESD) and effective dose (ED) were measured using a DAP meter (Kerma X_plus) and CALDose_X 5.0 Monte Carlo software, respectively. The second phase, an experimental study utilized an anthropomorphic phantom (PBU-50) and TOR CDR Leeds test object for comparison of image quality. In the optimization phase, the imaging parameters with acceptable image quality and lowest ESD from the experimental study were adjusted for patient's body thickness. Image quality was evaluated by two radiologists using the modified evaluation criteria score lists.

Results: A significant difference was observed between the pre- and post-optimization phases for all examinations for image quality. However, ESD was significantly different between the two phases for PA chest and AP abdomen. The ESDs for three of the examinations were lower than those reported in all published studies. The ESD and ED obtained for all examinations were lower than recommended by radiation regulatory bodies.

Conclusion: The optimization of image quality and dose was achieved by utilizing an appropriate tube potential, calibrated automatic exposure control, and additional filtration of 0.2 mm copper.

► *Please cite this article as:*
Moey SF, Shazli ZA. Optimization of Dose and Image Quality in Full-field Digital and Computed Radiography Systems for Common Digital Radiographic Examinations. Iran J Med Phys 2018; 15: 28-38.10.22038/ijmp.2017.25091.1255.

Introduction

Radiation is now firmly established as an essential tool for diagnostic and therapeutic purposes. The beneficial effects of radiology on patients arising from properly conducted procedures have resulted in the widespread use of this modality, which in turn increases the population exposure to the total medical radiation [1]. Patient radiation dose is determined by the required image quality and diagnosis. Clinically, the imaging process is influenced by the procedure and the numerous factors related to the imaging equipment.

Therefore, effort must be carried out to optimize factors affecting radiation dose and image quality consistent with the concept of as Low as Reasonably Achievable. The need to optimize radiation protection for patients without compromising the diagnostic image quality is emphasized in the International Commission on Radiation Protection (ICRP) publication 60 [2]. The use of radiology is justified when the clinical benefit of the imaging procedure outweighs the associated radiation risk [3].

Dose reduction and optimisation are different in digital radiography system, compared to those of screen-film radiography. Digital techniques have the potential to reduce patient doses; however, they are also able to significantly increase them since these systems have wider exposure latitude as well as greater dynamic range and post-processing abilities [4]. Therefore, awareness regarding the need to manage radiation dose is of significant importance as in digital systems, an overexposure can occur without an adverse impact on image quality.

Optimization is a balance between image quality and radiation dose; however, it does not signify minimizing patient dose and maximizing image quality [5]. The image quality required for making clinical diagnosis is determined by the radiologist. In

*Corresponding Author: Department of Diagnostic Imaging and Radiotherapy, Kulliyyah (Faculty) of Allied Health Sciences, International Islamic University Malaysia, Kuantan Campus, 25200 Kuantan, Pahang, Malaysia, Tel: +609-5713346, Fax: +609-5716776, Email: moeysf@iium.edu.my

this regard, the lowest radiation dose is ascertained without compromising the image quality [6].

Digital X-ray imaging is a technology that is rapidly advancing and will soon affect millions of patients. If steps are not taken with regards to radiation protection issues, patients' medical exposure will increase significantly, and they will receive no concurrent benefits in this respect. Although digital imaging systems are beneficial, they demand the induction of some changes in ways of working as they involve issues related to cost, productivity, the need to acquire new skills, radiation doses, issues of overuse, and image quality.

In order to optimize dose and image quality, we need to address the current safety issues with clinical digital radiography, which arise from human factors, such as inappropriate exposure, increased number of exposures, inadequate collimation, and image quality, which are incompatible with imaging tasks. The phenomena of dose creep in digital diagnostic imaging is referred to as the enhancement of patient radiation dose through excessive exposure overtime by the radiographers for ensuring an acceptable image quality [8]. Given the wide density and latitude in digital imaging, the radiographers often choose the path of least resistance by increasing exposure technique in the bid to decrease image noise and avoid repeats due to exposure settings [9].

With this background in mind, the present study was conducted with the aim of investigating dose optimization and image quality in four common digital imaging examinations. To this aim, we performed the optimization process for image quality and dose for common digital radiographic examinations so that the diagnostic value of the image was of acceptable quality without causing harmful effects on the patient that might result from ensued radiation exposures.

Materials and Methods

The study was undertaken in three phases.

Phase 1: Pre-optimization Study

The pre-optimization phase involved 90 physically able patients weighing 60-80 kg within the age range of 20-60 years. The study was carried out during March and May 2016 at Hospital Sultan Haji Ahmad Shah (HOSHAS), Pahang, Malaysia. Ethical approval (No: IIUM/305/14/11/2/IREC581) was obtained from the Research Ethics Committee of International Islamic University of Malaysia.

Estimation of dose and image quality was performed on four of the most common examinations carried out at the centre under investigation. These examinations included erect posterioanterior (PA) chest, anterioposterior (AP) abdomen, as well as AP and lateral lumbosacral spine. At this stage, the exposure parameters and radiographic technique were left to the discretion of the radiographers performing the examinations. The radiography of the AP abdomen as well as AP and lateral lumbosacral spine were performed by means of a Vertex Multixtop X-ray unit (Siemens, Germany) by using a barium fluoro bromide imaging plate activated with europium.

However, for the chest, full-field digital radiography (FFRD) was performed using direct digital detector, namely Axiom Aristos (Siemens, Germany), incorporating a cesium iodide-amorphus silicone flat panel detector. In addition, the entrance surface dose (ESD) was determined using a dose area product (DAP) meter (Kerma X_plus, IBA, Germany) that was placed beneath the collimator to cover the entire collimation area during the performance of the radiographic examination.

Dose Estimation

Effective dose (ED) was evaluated using the CALDose_X 5.0 Monte Carlo software, Department of Nuclear Energy, Federal University of Pernambuco, Brazil. The incident air kerma (INAK) was estimated based on the X-ray tube output curve, and the ESD was then calculated by multiplying this INAK value with the backscatter radiation factor. Conversion coefficient can be calculated individually for male adult phantom (MASH) and female adult phantom (FASH) using this software. The absorbed dose and ED for gender-specific organs and patient positioning can then be obtained together with cancer risk arising from the radiographic examination by means of the conversion factor. The ESD can be calculated by such exposure parameters as kilovoltage, tube current-time, and focus-film distance using the following equation [10]:

$$ESD = o \times (\frac{V}{80})^2 \times (\frac{100}{d})^2 CTf \quad (1)$$

Where f is the scatter factor, T is the exposure time in second, C is current in mA, d is the focus to skin distance in cm, V is tube voltage in kV, and O is the tube output in mGy/mAs.

Image Quality

Image quality was evaluated on the same sets of radiographs by two recruited radiologists blinded to the study using high contrast illuminator 1500 cd/m^2 based on the modified evaluation criteria scoring lists derived from the Commission of European Communities (CEC, 1996) [11]. Therefore, the evaluation of the image quality of the radiographs was based on the subjective visibility of specific anatomical structures on a score range of 1-4 for each criterion.

Depending on the number of criteria, the total score of image quality for each radiograph could range within 4-32. In this grading system, better image quality is indicated by higher scores. The criteria used in this grading system represented the radiographic features that were dependant on the employed radiographic technique.

Figure 1. Experimental set up for PA chest radiography

Phase 2: Experimental Study

Phase two involved an experimental (simulation) study targeted toward investigating the optimization of exposure and technical factors as a strategy for the management of radiation dose-image quality. The experimental study was conducted at the Radiography Laboratory, Department of Diagnostic Imaging and Radiotherapy, Kulliyyah of Allied Health Sciences, International Islamic University of Malaysia, Kuantan, Pahang. The X-ray was implemented using a Multixtop unit (Siemens, Germany) with a (43×35 cm) barium fluoro bromide imaging plate activated with europium.

The acquired image was read by a single read out image reader, namely FCR Capsula XLII (CR-IR 359), and then printed out using the Fuji Medical Dry Laser DRYPIX Plus (Model 4000, Fuji, Japan) for objective image quality scoring. The setup of the experimental study for the PA chest radiography is illustrated in Figure 1. The study utilized an anthropomorphic phantom (PBU-50) and TOR CDR Leeds test object (Leeds Test Objects Limited, United Kingdom) for the relative comparison of the obtained image quality.

The whole body PBU-50 is a life-size, full body anthropomorphic (Kyotokagaku, Japan) phantom with the newest synthetic lungs, liver, kidneys, skeleton, and mediastinum encased in soft tissue substitute. The ESD was determined using a DAP meter (Kerma X_plus, Iba Dosimetry, Germany), which was inserted beneath the collimator to cover the whole collimated area during the radiographic examination. Image acquisitions were carried out for the four common radiographic examinations, erect PA chest, AP abdomen, as well as AP and lateral lumbosacral spine using the specified imaging parameters (tables 1, 2, 3, and 4).

Table 1. Imaging parameters used for the erect posterioanterior chest

Imaging parameters	Details
Imaging plate size (cm)	35×43 lengthwise
Source to image distance (cm)	180
Grid (grid ratio)	Moving grid, 12:1
Kilovoltage peak (kVp)	99, 105, 109, 117, 121, 125
Central ray	Perpendicular to the center of IR, mid sagittal plane at the level of T7
Additional filtration	No filter, 1 mm Al, 2 mm Al, 0.1 mm Cu, 0.2 mm Cu
Focal spot	Large focal spot (1.0 mm)
Chamber	Side chambers
Automatic exposure control	On (0)

Table 2. Imaging parameters used for the anterioposterior abdomen

Imaging parameters	Details
Imaging plate size (cm)	35×43 lengthwise
Source to image distance (cm)	100, 110, 120
Grid (grid ratio)	Moving grid, 12:1
Kilovoltage peak (kVp)	70, 75, 81, 85, 90
Central ray	Perpendicular to the center of IR at the level of the upper border of the iliac crest
Additional filtration	No filter, 1 mm Al, 2 mm Al, 0.1 mm Cu, 0.2 mm Cu
Focal spot	Large focal spot (1.0 mm)
Chamber	Side chambers
Automatic exposure control	On (0)

Table 3. Imaging parameters used for the anterioposterior lumbosacral spine

Imaging parameters	Details
Imaging plate size (cm)	35×43 lengthwise
Source to image distance (cm)	100, 110, 120
Grid (grid ratio)	Moving grid, 12:1
Kilovoltage peak (kVp)	70, 75, 81, 85, 90
Central ray	Perpendicular to the center of IR, mid sagittal plane level of L3
Additional Filtration	No filter, 1 mm Al, 2 mm Al, 0.1 mm Cu, 0.2 mm Cu
Focal spot	Large focal spot (1.0 mm)
Chamber	Middle chamber

Automatic exposure control	On (0)

Table 4. Imaging parameters used for the lateral lumbosacral spine

Imaging parameters	Details
Imaging plate size (cm)	35×43 lengthwise
Source to image distance (cm)	100, 110, 120
Grid (grid ratio)	Moving grid, 12:1
Kilovoltage peak (kVp)	81, 85, 90, 96, 102
Central ray	Perpendicular to the center of IR, coronal plane, level of L3
Additional Filtration	No filter, 1 mm Al, 2 mm Al, 0.1 mm Cu, 0.2 mm Cu
Focal spot	Large focal spot (1.0 mm)
Chamber	Middle chamber
Automatic exposure control	On (0)

Table 5. Parameters of the phantom study with the lowest entrance surface dose and acceptable image quality adapted for the optimization study

Variables	PA Chest		AP Abdomen		AP Lumbosacral		Lateral Lumbosacral	
	Phantom	Patient	Phantom	Patient	Phantom	Patient	Phantom	Patient
kVp	125	125	81	81	81	81	85	85
Thickness (cm)	27	27	26	26	26	26	32	32
Gender**	Male	Male	Male	Male/Female	Male	Male/Female	Male	Male/Female
Filter (Cu in mm)	0.2	0.2	0.2	0.2	0.2	0.2	0.2	0.2
FFD	180	180	115	115	115	115	115	115
AEC (Chamber)	2 Sides	2 Sides	2 Sides	2 Sides	Centre	Centre	Centre	Centre

** Female 27 cm AP thickness – 113 kVp (PA Chest Only)
PA: posterioanterior, AP: anterioposterior, FFD: focus to film distance, AEC: automatic exposure control

A total of 288 images (72 images for each of the examinations) were evaluated based on the imaging parameters shown in tables 1, 2, 3, and 4 for acceptable image quality by determining the number of small (high-contrast detectability) and large disks (low-contrast detectability) as well as the group of resolution test patterns visualized when using each of the imaging parameters. The fine balance of image quality and dose was determined for each of the projection by choosing the imaging parameter with the lowest ESD and acceptable image quality (Table 5).

Phase 3: Post-optimization study

The imaging parameters with the lowest ESD and acceptable image quality obtained from the experimental study were then adjusted for patient size for the optimization study by means of a phantom. Table 5 illustrates the parameters of the phantom study with the lowest ESD and acceptable image quality along with those used in the optimization study. Before the initiation of optimization, a continuous medical education session was implemented for all radiographers in the department. This session was held with the aim of informing them about radiography faults and corrective actions that had to be taken during the post-optimization study.

The post-optimization study was carried out on 90 patients (i.e., 30 cases for each of the PA chest, AP abdomen, as well as AP and lateral lumbar sacral spine) to determine dose and image quality. The patients included in this phase met the criteria stated in the pre-optimization stage using the same X-ray unit and image acquisition parameters. The results of the post-optimization study were then compared to those of the pre-optimization study for the four common examinations. A change of 2kVp for each centimeter of anatomical thickness [12] was applied in the optimization study.

Statistical Analysis

As the data violated the stringent assumptions of the paired sample t-test, Wilcoxon test was employed to test for the difference between pre- and post-optimization in terms of image quality and radiation dose. In addition, Cohen's kappa coefficient was used to rate inter-observer agreement for overall scores of image quality. Data analysis was performed using SPSS, version 18.

Results

Patients' Demographic Data and Technique Parameters

Patients' demographic data and technique parameters for the pre- and post-optimization of the PA chest, AP abdomen, as well as AP and lateral lumbosacral spine are presented in tables 6, 7, 8, and 9, respectively. The data obtained from the four radiographic examinations were also compared to those reported in other studies.

Table 6. Summary of patients' demographic characteristics and technical parameters used for the posterioanterior chest in Hospital Sultan Haji Ahmad and other studies

Variables	This Study		Other studies			
	PRE OP	POST OP	Asadinezhad & Toossi, 2008[13]	Abdullah et al., 2010[14]	Hart et al., 2010[15]	Osei & Darko, 2012[16]
	Mean (Range)	Mean (Range)	Mean (Range)	Mean (Range)	Mean (Range)	Mean (Range)
Age	46.3 (21-60)	42.13 (23-60)	45 (18-80)	47 (18-690	68 (16-97)	60.1 (15-88)
Weight (kg)	65.6 (57-80)	68.5 (60-80)	68 (52-88)	65 (36-101)	70 (49-93)	NA
kVp	121.5 (121-129)	112.7 (102-129)	66 (46-83)	65 (56-72)	88 (62-104)	119 (70-129)
mAs	1.57 (0.97-2.59)	2.32 (1.02-3.72)	18 (4-90)	5 (4-10)	5 (0.3-405)	5.4 (1.14-18)
Total Filtration	2.5 mm Al + 0.2 mm Cu	2.5 mm Al + 0.2 mm Cu	(2-3.5 mm Al)	(2-3.05 mm Al)	2.8 mm Al (2.5-3.3 mm Al)	NA
Collimation size (m)	0.11 (0.09-0.12)	0.104 (0.08-0.19)	NA	NA	NA	NA
System	FFDR (direct)	FFDR (direct)	SF (400s)	SF	SF (400s)	SF
Types of patient	Ambulatory patient	Ambulatory patient	Ambulatory patient	Ambulatory patient	Ambulatory patient	Ambulatory patient
AEC	Side chamber	Side chamber	Side chamber	Side chamber	Side chamber	Side chamber
FFD (cm)	180	180	NA	NA	NA	NA
S-value	177±39.2	181.47±36.8	NA	NA	NA	NA

PRE OP: pre-optimization, POST OP: post- optimization, FFDR: full-field digital radiography, SF: screen-film, AEC: automatic exposure control, FFD: focus to film distance

Table 7. Summary of patients' demographic characteristics and technical parameter used for the anterioposterior abdomen in Hospital Sultan Haji Ahmad and other studies

Variables	This study		Other studies			
	PRE OP	POST OP	Aliasgharzadeh et al., 2015[17]	Osei & Darko, 2012[16]	Hart et al., 2010[15]	Abdullah et al. 2010[14]
	Mean (Range)	Mean (Range)	Mean (Range)	Mean (Range)	Mean (Range)	Mean (Range)
Age	41.63 (23-60)	46.43 (20-60)	NA	60.5 (25-89)	NA	51 (30-69)
Weight (kg)	66.3 (60-80)	69.4 (60-80)	NA	NA	NA	63 (39-88)
kVp	74.87 (70-81)	80.25 (70-90)	73	87.6 (65-90)	76	72 (63-88)
mAs	40.5 (12-98)	43.42 (10.6-72)	24	34.4 (10-121)	41	35 (20-50)
Total filtration	2.5 mm Al	2.5 mm Al + 0.2 mm Cu	(2-3.5 mm Al)	NA	3.1 mm Al (2.6-3.6 mm Al)	(2-3.05 mm Al)
Collimation size (m)	0.180 (0.09-0.12)	0.147 (0.14-0.16)	NA	NA	NA	NA
System	CR	CR	SF	SF	SF	SF
Types of patient	Ambulatory patient	Ambulatory patient	Ambulatory patient	Ambulatory patient	Ambulatory patient	Ambulatory patient
AEC	Side Chamber	Side Chamber	Side Chamber	Side Chamber	Side Chamber	Side Chamber
FFD (cm)	108.4 (102-115)	115.2 (115-118)	NA	NA	NA	NA
S-value	246.54±89.9	264.73±66.7	NA	NA	NA	NA

PRE OP: pre-optimization, POST OP: post- optimization, CR: computed radiography, SF: screen-film, AEC: automatic exposure control, FFD: focus to film distance

Table 8. Summary of patients' demographic characteristics and technical parameters used for the anterioposterior lumbosacral in Hospital Sultan Haji Ahmad and other studies

Variables	This Study		Other studies			
	PRE OP	POST OP	Aliasgharzadeh et al., 2015[17]	Osei & Darko, 2012[16]	Hart et al., 2010[15]	Abdullah et al. 2010[14]
	Mean (Range)	Mean (Range)	Mean (Range)	Mean (Range)	Mean (Range)	Mean (Range)
Age	41.83 (22-60)	44.8 (20-60)	NA	56.6 (14-84)	NA	49 (23-72)
Weight (kg)	67.72 (60-80)	66.9 (60-80)	NA	NA	NA	68 (44-138)
Kvp	77.11 (70-87.5)	80.7 (70-110)	74	87.4 (80-110)	78	73 (68-90)
mAs	51.17 (22-182)	66.47 (20-241)	24	90.1 (12.3-187)	46	35 (25-63)
Total filtration	2.5 mm Al	2.5 mm Al + 0.2 mm Cu	(2-3.5 mm Al)	NA	3.1 mm Al (2.6-3.6 mm Al)	(2-3.05 mm Al)
Collimation size (m)	0.1271 (0.094-0.216)	0.08 (0.06-0.093)	NA	NA	NA	NA
System	CR	CR	SF	SF	SF	SF
Types of patient	Ambulatory patient	Ambulatory patient	Ambulatory patient	Ambulatory patient	Ambulatory patient	Ambulatory patient
AEC	Mid chamber	Mid chamber	Mid chamber	Mid chamber	Mid chamber	Side chamber
FFD (cm)	114.93 (113-115)	115 (-)	NA	NA	NA	NA
S-value	335.9±252	181.2±89.3	NA	NA	NA	NA

PRE OP: pre-optimization, POST OP: post- optimization, CR: computed radiography, SF: screen-film, AEC: automatic exposure control, FFD: focus to film distance

Table 9. Summary of patients' demographic characteristics and technical parameters used for the lateral lumbosacral in Hospital Sultan Haji Ahmad and other studies

Variables	This Study		Other studies			
	PRE OP	POST OP	Aliasgharzadeh et al., 2015[17]	Osei & Darko, 2012[16]	Hart et al., 2010[15]	Abdullah et al., 2010[14]
	Mean (Range)	Mean (Range)	Mean (Range)	Mean (Range)	Mean (Range)	Mean (Range)
Age	41.83 (22-60)	44.8 (20-60)	NA	59.2 (14-84)	NA	45 (17-72)
Weight (kg)	67.72 (60-80)	66.9 (60-80)	NA	NA	NA	72 (44-138)
kVp	84.23 (70-99)	87.62 (75-120)	82 (N/A)	97.3 (90-110)	89 (N/A)	85 (74-93)
mAs	59.78 (28-215)	99.6 (14.4-308)	40 (N/A)	108.5 (27.7-243)	56 (N/A)	52 (32-80)
Filtration	2.5 mm Al	2.5 mm Al + 0.2 mm Cu	2-3.5 mm Al	NA	3.1 mm Al (2.6-3.6)	2-3.05 mm Al
Collimation size (m)	0.1393 (0.11-0.206)	0.08 (0.055-0.093)	NA	NA	NA	NA
System	CR	CR	SF	SF	SF	SF
Types of patient	Ambulatory patient	Ambulatory patient	Ambulatory patient	Ambulatory patient	Ambulatory patient	Ambulatory patient
AEC	Mid chamber	Mid chamber	Mid chamber	Mid chamber	Mid chamber	Mid chamber
FFD (cm)	115	115	NA	NA	NA	NA
S-value	436.7±183	297±106	NA	NA	NA	NA

PRE OP: pre-optimization, POST OP: post- optimization, CR: computed radiography, SF: screen-film, AEC: automatic exposure control, FFD: focus to film distance

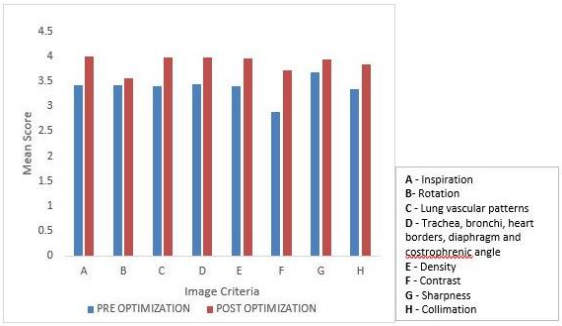

Figure 2. Mean image quality score for pre and post optimization for PA chest

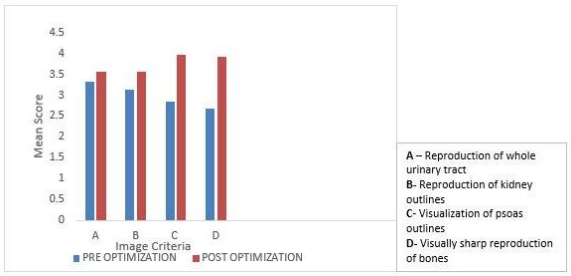

Figure 3. Mean image quality score for pre and post optimization for AP abdomen

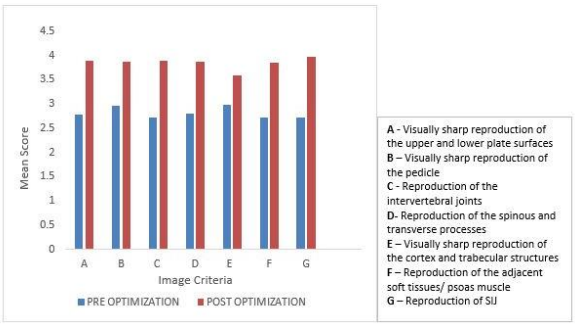

Figure 4. Mean image quality score for pre and post optimization for AP lumbosacral spine

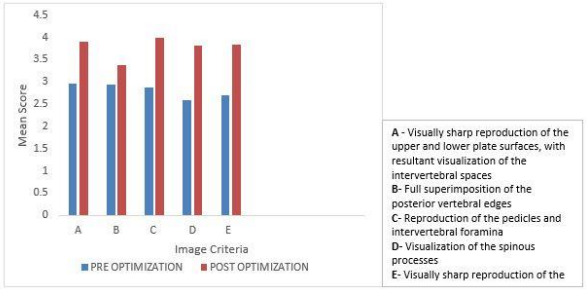

Figure 5. Mean image quality score for pre and post optimization for lateral lumbosacral spine

Image Quality

Image assessment and analysis were carried out on 240 radiographs (i.e., 120 and 120 images obtained in the pre- and post-optimization phases for the four radiographic examinations, respectively). The radiographs were assessed for obtained image quality using the aforementioned technique parameters. The assessors' mean scores for positioning and radiographic technique are summarized in figures 2, 3, 4, and 5 for the four examinations.

Inter-observer Agreement

A high inter-observer agreement was achieved regarding the overall image quality scores of the four radiographic examinations for the pre- and post-optimization. The Cohen's kappa coefficients were 0.77 and 0.9 for the PA chest in the pre-and post-optimization phases, respectively. In terms of the AP abdomen, a high agreement was obtained for the pre- and post-optimization, rendering Cohen's kappa coefficients of 0.83 and 0.84, respectively.

Similar high inter-observer agreement coefficients were observed for the pre- and post-optimization regarding the AP lumbosacral spine, which were 0.84 and 0.83, respectively. In addition, considering the lateral lumbosacral spine, the Cohens' kappa coefficients were 0.89 and 0.81 for the pre- and post-optimization phases, respectively.

Entrance Surface Dose and Effective Dose

The summary of the ESD derived from the four routine radiographic examinations for the pre- and post-optimization and other published data are shown in Table 10. In addition, the guidance levels for ESD and ED for the four radiographic examinations obtained from various agencies are displayed in tables 11 and 12, respectively.

Statistical Analysis

Image Quality

The results of the Wilcoxon signed-rank test revealed a significant difference between the pre- and post-optimization phases for the PA chest ($Z=-4.788$, $P<0.05$), AP abdomen ($Z=-4.638$, $P<0.05$), AP lumbosacral spine ($Z=-4.79$, $P<0.05$), and lateral lumbosacral spine ($Z=-4.547$, $P<0.05$) radiographic examinations in terms of image quality. Accordingly, for all four examinations the image quality was better in the post-optimization phase, compared to that in the pre-optimization one.

Entrance Surface Dose

According to the results of the Wilcoxon signed-rank test, there was a significant difference in the ESD obtained in the pre- and post-optimization stages for the PA chest ($Z=-3.723$, $P<0.05$) and AP abdomen ($Z=-2.293$, $P<0.05$). In this regard, the ESD estimated in the post-optimization was lower than that of the pre-optimization phase. Regarding the AP abdomen, a significant difference was observed in the ESD between the pre- and post-optimization phases ($Z=-2.293$). In this respect, the ESD was lower in the post-optimization than that in the pre-optimization phase. However, ESD showed no significant difference between the pre- and post-optimization for the AP and lateral lumbosacral spine radiographic examinations.

Table 10. Comparison of entrance surface dose (in mGy) derived from routine radiographic examinations for pre- and post-optimization between Hospital Sultan Haji Ahmad and other published studies

Examination	This Study		Hart et al., (2010)[15]	Abdullah et al., 2010[14]	Osei & Darko, 2012[16]	Aliasgharzadeh et al., 2015[17]
	PRE OP Mean (S.D)	POST OP Mean (S.D)				
Chest (PA)	0.098±0.06	0.0195±0.05	0.15	0.18	0.14	0.37
Abdomen (AP)	2.57±1.64	1.53±0.975	4	4.89	1.82	2.01
Lumbosacral (AP)	2.650±1.42	2.631±2.02	5.7	5.74	3.72	2.18
Lumbosacral (LAT)	3.75±2.59	3.66±1.68	10	11.36	6.28	5.36

PRE OP: pre-optimization, POST OP: post- optimization, PA: posterioanterior, AP: anterioposterior, LAT: lateral

Table 11. Guidance levels for entrance surface dose (in mGy) as prescribed by various agencies for four routine radiographic examinations

Radiograph	Projection	IAEA[18]	CEC (1996)[11]	UK (2010)[15]	Malaysia (1998)[19]	UNSCEAR (2008)[20]
Chest	PA	0.4	0.3	0.15	0.28	0.33
Abdomen	AP	10	-	4	10	3.64
Lumbo sacral	AP	10	10	5	10.56	4.07
Lumbo sacral	LAT	30	30	11	18.60	8.53

PA: posterioanterior, AP: anterioposterior, LAT: lateral

Table 12. Guidance levels for effective dose (in mSv) as prescribed by various agencies for four routine radiographic examinations

Examination	This study (Optimization)	UNSCEAR (2008)[21]	U.K E-60[22]	U.K E-103[22]
Chest (PA)	0.0062	0.05	0.014	0.014
Abdomen (AP)	0.148	0.8	0.47	0.43
Lumbosacral (AP)	0.189	1.2	0.41	0.39

UNSCEAR: United Nations Scientific Committee on the Effects of Atomic Radiation, PA: posterioanterior, AP: anterioposterior

Discussion

Patients' Demographics and Technical Parameters

Posterior Anterior Chest Radiography

Similarities of data for the present study to that of other studies include types of patient in which all studies use only ambulatory patients. Age of patients in this study was similar to that of patients used in the study conducted by Asadinezhad and Toosi (2008) and Abdullah et al. (2010). The study by Hart et al. (2010) and Osei and Darko (2012) however employed older patients with a mean age of 68 years and 60.1 years respectively. The mean weight of patients when comparing the present study to other studies were quite similar between 65-70 kilogram but the range of patients' weight for the study conducted by Abdullah et al. (2010) and Hart et al. (2010) were 36 -101 kilogram and 49 -93 kilograms respectively.

In terms of mean tube potential, this study (post optimization) utilized high kVp technique, 112.7kVp (range 102-129kVp) as opposed to that of the medium kVp range utilized by Asadinezhad and Toosi (2008), Abdullah et al. (2010) and Hart et al. (2010). Despite a high kVp of 119kVp utilized by Osei and Darko (2012), the range of kVp used was between 70 kVp-129 kVp. An additional 0.2mm Cu was added to the inherent filtration of 2.5mm Al equivalent for the present study. However other studies utilized total filtration of between 2-3.5 mm Al equivalent. Further, direct radiography utilizing cesium iodide amorphous silicon detector was employed in the current study in contrast to other studies that utilized screen-film with 400 film speed. However, all studies utilized the AEC.

Anterior Posterior Abdomen Radiography

The age of the patients utilized in the study was younger than that for the studies carried out by Osei and Darko (2012) and Abdullah et al. (2010). However, despite the fairly similar weight of patients in the current study to that of the study by Abdullah et al (2010), the patients' weight range was big (39-88 kilogram). The patients employed in all the studies were ambulatory patients.

The mean tube potential utilized for the present study (post optimization) at 80 kVp is higher than that employed by Aliasgharzadeh et al. (2015), Hart et al. (2010) and Adullah et al. (2010) but lower than that utilized by Osei & Darko (2012). The current study utilized an inherent filtration of 2.5mm Al equivalent with an additional 0.2mm Cu. However other studies utilized a total filtration of between 2-3.5mm Al equivalent. The AEC were utilized in all the studies. However, the current study employed

computed radiography as opposed to that of screen-film technology in all other studies.

Anterior Posterior Lumbosacral Spine

Patients' mean age for the study and that by Abdullah et al (2010) were between 42-49 years. However, the mean age of patients for the study carried out by Osei and Darko (2012) was older at 57 years. The mean weight of the patients for this study and other studies were between 67-68 kilograms and all patients were ambulatory patients.

The mean tube potential utilized by the current study (post optimization) at 81kVp was higher than the study conducted by Aliasgharzadeh et al. (2015), Hart et al. (2010) and that by Abdullah et al. (2010) but is lower than that utilized by Osei & Darko (2012). The total tube filtration for the present study (post optimization) utilized inherent filtration of 2.5mm Al equivalent with an added 0.2mm Cu. However other studies used total filtration of between 2-3.5mm Al equivalent. Further computed radiography was utilized for the current study compared to that of other studies which employed screen-film technology.

Lateral Lumbosacral Spine

The mean age of patients for the present study and that by Abdullah et al. (2010) ranged from 42-45 years. However, the study by Hart et al. (2010), the mean age of the patients was 59 years. All patients in all the studies were ambulatory patients. The mean weight of the patients utilized in the study ranged from 67-72 kilograms.

The mean tube potential employed in the current study at 88kVp was similar to that by Hart et al. (2010) but was slightly higher than that utilized in the study carried out by Aliasgharzadeh et al. (2015) and Abdullah et al. (2010). However, the tube potential used by Osei and Darko (2012) at 97 kVp was higher than the current study. The present study used total filtration of 2.5mm Al equivalent filtration with an additional 0.2mm Cu. Other studies employed total filtration of between 2-3.5mm Al equivalent. Further all studies employed the AEC. Image acquisition for the current study utilized computed radiography whereas other studies used the screen-film technology.

Image Quality

In the present study, we compared ESD and image quality scores obtained in the pre- and post-optimization phases for the four common radiographic procedures using the same X-ray unit, but different technical parameters. According to the findings, there was a significant difference between the pre- and post-optimization phases for all four radiographic examinations in terms of the image quality. Image quality was determined by selecting the tube potential (kVp) appropriate for the required contrast and thickness of the anatomy.

The factors pertaining to variation in image detector phosphor sensitivity of cesium iodide in FFDR direct digital detector and barium fluoro bromide phosphors in computed radiography (CR) in terms of absorbed photon energy and tube potential were given due consideration. As a result, a digital image of diagnostic quality with sufficient penetration (kVp) and adequate mAs was produced with minimum quantum mottle aided by a calibrated automatic exposure control (AEC) [23]. The consideration of proper alignment with essential anatomy in the image facilitated the achievement of more effective collimation.

This aided in reducing the scatter from reaching the image receptor, which resulted in improved image contrast. This can be seen in the improvement of image contrast score from 2.88 to 3.73 for the PA chest. Radiation quality, which is determined by the selected tube potential and the filtration of the X-ray beam, was augmented in this study by using a 0.2 mm copper additional filtration.

This was done to attenuate the photons with lower energy that were unlikely to reach the image receptor. This measure further influenced the X-ray beam quality affecting the balance of signal-to-noise ratio and patient dose resulting from the interaction of X-ray photons and tissue [23]. This was probably the main reason explaining the significant improvement of image quality for all four radiographic examinations in this study.

Image quality was further enhanced before optimization by the implementation of a continuous medical education for the radiographers targeted toward highlighting the importance of proper and accurate positioning of the anatomy to cover the AEC detectors. Adherence to the optimization protocols and exposure technique regarding AEC application assisted in ensuring the proper administration of digital radiography.

This facilitated a consistent exposure to the image receptor and resulted in an image of diagnostic quality [24]. Exposure technique charts established by the study eliminated the concerns and confusions associated with the appropriate use of such technique parameters as kVp, mA, focus to film distance (FFD), and grid use.

Entrance Surface Dose and Effective Dose

The comparison of the ESD obtained for the pre- and post-optimization phases revealed significant differences between the two phases for all four radiographic examinations. This could be the result of using an appropriate tube potential in line with the sensitivity of phosphor used in FFDR and CR. Additionally, the effective collimation in the post-

optimization phase resulted in reduced ESD for the PA chest and AP abdomen examinations.

The insignificant difference in the ESD obtained for the pre- and post-optimization of the AP and lateral lumbosacral spine could be ascribed to the use of added filtration of 0.2 mm copper. The absorption of the low energy photons (20-50 keV) by the copper filter necessitated increasing the tube output at 80 kVp by as much as 50% [25].

This then will affect the exposure time when using the AEC. Another possible reason for this insignificant change was the exposure time set by the radiographer that was shorter than the minimum response time (MRT) of the AEC due to the selection of high mA for some of the lumbosacral radiographic examinations. As the shortest exposure time corresponded to the MRT, this will result in a higher exposure time [12], and therefore a higher mAs will result in a higher ESD.

The utilization of 115 cm FFD that corresponded to that of the focus to grid distance for the X-ray unit (FFD recommended by Siemens) in the optimization phase further aided in the reduction of ESD for the AP abdomen (Table 7). The most important parameter affecting the AEC and ESD is the FFD, which in this case using the inverse square necessitated the increase in the radiographic exposure to obtain the same optical density on the radiograph. Due to grid "cut-off," in this scenario, even though the FFD was increased, the ESD was significantly reduced.

In this respect, the grid cutoff in the pre-optimization phase for the AP abdomen would possibly lead to the absorption of the X-ray photons by the slanted lead strips of the grid [24] resulting in more exposure that is required to reach the image receptor, and thereby the AEC. This resulted in recording a higher mAs, and consequently higher ESD.

Regarding the AP and lateral lumbosacral spine examinations, there were differences in the ESD between the pre- and post-optimization; nonetheless, the differences were not significant. This would possibly be the result of insignificant difference in the FFD used in the pre- and post-optimization for these two radiographic examinations (tables 8 and 9). Furthermore, there was also insignificant grid cutoff as the FFD was in accordance to the focus-grid distance recommended by the manufacturer.

The comparison of the mean ESD obtained during optimization in the present study to that of other studies indicated the employment of a higher tube potential in this study as compared to that in other studies resulted in a lower mAs. This then resulted in the achievement of a lower ESD. Furthermore, in the present study, we employed FFDR direct digital detector for the PA chest radiography and CR for the AP abdomen and AP and lateral lumbosacral spine as opposed to other studies using screen-film.

However, the types of intensifying screen were not specified in the other studies. Generally, cesium iodide used in the flat plate detector for FFDR in the chest radiography is more sensitive due to the thicker phosphor in its construction, compared to those used in CR or screen-film. Moreover, due to the higher sensitivity of barium fluorohalide used in CR, compared with gadolinium oxysulfide used in SF, radiation exposure has to be increased from 30% to 40% to compensate for its lower sensitivity, and therefore a higher ESD is obtained ~~used~~ in screen-film combination [25].

The comparison of this study in HOSHAS and other published studies in terms of the ESD during post-optimization indicated that the ESDs for the PA chest, AP abdomen, as well as AP and lateral lumbosacral spine examinations were lower for this study in HOSHAS than those reported in the other studies (Table 10). Nonetheless, regarding the AP abdomen, the ESD for this study in HOSHAS was slightly higher than that obtained in a study performed by Aliasgharzadeh [17].

However, when comparing the ESD estimated in the present study with the guidelines established by the radiation regulatory bodies (Table 11), the ESD attained in this study for all four radiographic examinations were lower than the recommended values. In addition, the ED obtained for HOSHAS for the four radiographic examinations suggested a lower dose than that found in the guidelines (Table 12).

Conclusion

In the present study, we optimized dose and image quality by employing an appropriate tube potential in relation to the sensitivity of the phosphor used in the imaging receptor. Additionally, the proper usage of AEC and radiographic technique further aided the post-optimization process. Higher tube potential was utilized for thicker parts of the anatomy, and adjustments were made for body thickness to eliminate high patient dose.

The results of the study indicated that the incorporation of 0.2 mm copper into the X-ray unit facilitated the reduction of ESD for all four examinations despite utilizing an increased tube output. The ESDs obtained in this study for the PA chest, AP abdomen, as well as lateral lumbosacral spine were lower than those reported by other studies. However, the ESDs and EDs for all four radiographic examinations obtained in this study were lower, compared to those published by radiation regulatory bodies and guidelines of radiation agencies.

Acknowledgment

The appreciation goes to all staff and also patients of the Diagnostic Imaging Department, HOSHAS, Temerloh, Malaysia. We also gratefully acknowledge the contribution of the radiologists from the Breast Imaging Centre, International Islamic University Malaysia, and Hospital Kuala Lumpur for evaluating the image quality of the radiographs.

References

1. International Atomic Energy Agency 2012. Proceedings series radiation protection in medicine: Setting the scene for the next decade proceedings of an international conference organized by IAEA. 3-7 December.
2. International Commission on Radiological Protection 1991. 1990 Recommendations of the International Commission on Radiological Protection. ICRP Publication 60. Ann. ICRP 21 (1-3).
3. United Nations Scientific Committee 2000. The effects of atomic radiation: Sources and effects of ionizing radiation. Geneva: UNSCEAR.
4. Vano E, Fernandez JM, Ten JI, Prieto C, Gonzalez L, Rodriquez R , et al. Transition from screen-film to digital radiography: Evolution of patient radiation doses at projection radiography. Radiology. 2007; 243(2): 461-6. DOI: 10.1148/radiol.2432050930.
5. Masoud OA, Muhogara WE , Msaki PK. Assessment of patient dose and optimization levels in chest and abdomen CR examinations at referral hospitals in Tanzania. Journal of Applied Clinical Medical Physics. 2015;16(5): 435-41. DOI: 10.1120/jacmp.v16i5.5614.
6. Ng KH. Ensuring safety in transition to digital radiography in practice. IAEA International Conference on radiation protection in medicine: Setting scene for the decade. 2013:223.
7. International Commission on Radiological Protection. Publication 93. Managing patient doses in digital radiology. Ann. ICRP 34 (1), 2004.
8. International Atomic Energy Agency 1996. International basic safety standards against ionizing radiation and for the safety of radiation sources. Vienna: IAEA.
9. Seeram E, Davidson D, Bushong S and Swan H. Optimizing the exposure indicator as a dose management strategy in computed radiography. Radiologic Technology. 2016; 87(4): 380-91.
10. Davies M, McCallum H, Whiter G, Brown J, Helm M. Patient dose audit in diagnostic radiography using custom designed software. Elsevier. 1997; 3(1): 17-25. DOI: 10.1016/S1078-8174(97)80021-1.
11. European Commission. European guidelines on quality criteria for diagnostic radiographic images. Luxembourg: European Commission; 1996. EUR 16260EN.
12. Ching W, Robinson J , McEntee M. Patient based radiographic exposure factor selection: a systematic review. Journal of Medical Radiation Sciences. 2014; 61(3): 176-90.
13. Asadinezhad M , Toosai MTB. Doses to patients in some routine diagnostic x-ray examinations in Iran: proposed the first Iranian diagnostic reference levels. Radiat prot dosimetry. 2008; 132(4): 409-14. DOI: 10.1093/rpd/ncn308.
14. Abdullah MHRO, Kandaiya S, Lim TH , Chumiran SH. Preliminary study on the trend of patient dose arising from diagnostic x-ray examinations in Penang, Malaysia. Journal of Applied Sciences Research. 2010; 6(12): 2257-63.
15. Hart D, Hillier M , Shrimpton P. HPA CRCE-034. Doses to patients from radiographic and fluoroscopic x-ray imaging procedures in the UK-2010 review.
16. Osei EK & Darko J. A survey of organ equivalent and effective doses from diagnostic radiology procedures. ISRN Radiol. 2013; 204346. DOI: 10.5402/ 2013/ 204346.
17. Aliasgharzadeh A, Mihandoost E, Masoumbeigi M, Salimian M , Mohseni M. Measurement of entrance skin dose and calculation of effective dose for common diagnostic x-ray examinations in Kashan, Iran. Global Journal of Health Science. 2015; 7(5): 202-7. DOI: 10.5539/gjhs.v7n5p202.
18. International Atomic Energy Agency/Commission of the European Communities 1995. Radiation dose in diagnostic radiology and methods for dose reduction IAEA-TECDOC-796 (Brussels: CEC).
19. Ng, KH, P Rassiah, HB Wang, AS Hambali, P Muthuvellu , HP Lee. Doses to patients in routine X-ray examinations in Malaysia. Br. J. Radiol. 1998; 71: 654-60.
20. United Nations Scientific Committee Atomic Radiation. Sources and effects of ionizing radiation: UNSCEAR 2008 Report to the General Assembly with scientific annexes (Vol. 1). New York United Nations Publications.
21. Muhogara WE, Ahmed NA, Almosabihi A, Alsuwaidi JS, Beganovic A, et al. Patient doses in radiographic examinations in 12 countries in Asia, Africa and Eastern Europe: initial results from IAEA projects. AJR Am J Roentgenol. 2008; 190(6): 1453-61. DOI: 10.2214/AJR.07.3039.
22. Wall B, Haylock R, Jansen J, Hillier M, Hart D , Shrimpton P. Radiation risks from medical x-ray examinations as a function of the age and sex of the patient. Health Protection Agency Centre for Radiation, Chemical and Environmental Hazards. 2011.
23. Martin CJ. Optimization in general radiography. Biomed Imaging Interv. Journal. 2007; 3(2). DOI: 10.2349/biij.3.2.e18.
24. Herrmann TL, Fauber TL, Gill J, Hoffman C, Orth DK, Peterson PA, et al. Best practices in digital radiography. Radiol Technol. 2012; 84:83–9.
25. Martin CJ. The importance of radiation quality for optimization in radiology. Biomed Imaging Interv Journal. 2007; 3(2). DOI: 10.2349/biij.3.2.e38.